Final Report Summary

Company Name:	Particle Beam Lasers, Inc.
Project Title:	Development of an accelerator-quality high-field common-coil dipole magnet
Principal Investigator:	Ronald M. Scanlan
Topic Number/Subtopic Letter:	27b

Research Carried Out and Research Findings:

To search beyond the Higgs requires particle accelerators of unprecedented energy, requiring dipoles of very high field to bend the particle beam to the desired radius. This SBIR project advanced a new approach and technology for building high-field dipoles based on the common-coil design. Because of the inherent simplicity and conductor-friendly nature of the design, the common-coil magnets are likely to be less expensive and easier to manufacture than the more-conventional cosine-theta magnets, particularly for high fields that require the use of brittle conductors such as Nb_3Sn.

Although several dipoles based on the common-coil design have been built, none had the high field quality required for accelerator magnets. During Phase I, we developed several designs for 16-T Nb_3Sn dipoles that in addition to other advantages met the field-quality requirements as specified for the proposed Future Circular Collider (FCC) with appealing configurations of pole coils. In fact, the type of designs developed during Phase I are already being adopted in common-coil magnet designs at various places in the world to achieve significant improvements in performance.

Phase I also prepared us for Phase II, where we will fabricate the most-promising configuration of pole coil and integrate it with the existing common-coil magnet DCC017 at BNL for a proof-of-principle demonstration of the design. Such a task is possible within the budget of an SBIR/STTR, as demonstrated in another PBL/BNL Phase II effort, because the magnet requires no expensive and time-consuming disassembly and reassembly to accommodate new coils. Based on this experience, another deliverable of Phase II will be a preliminary engineering design of a 16 T common-coil dipole that minimizes cost, provides an adequate support structure to withstand the Lorentz forces associated with these high fields, and is able to be built industrially in large numbers. Our effort will primarily be based on the low-temperature superconductor Nb_3Sn.

Potential Applications of the Research:

Not only is the common-coil design uniquely suited to building lower-cost, reliable high-field magnets for multi-billion-dollar colliding-beam particle accelerators such as FCC, commercial superconducting magnets also may benefit from the high-field technology developed: 1) methods for achieving good field quality; and 2) methods for supporting the superconductor against the large Lorentz forces experienced in high-field magnets. High-quality, high-field magnets will find commercial use in applications that include magnetic resonance imaging, proton and ion-beam therapy, wind power, and superconducting magnet energy storage.

I. FINAL SCIENTIFIC/TECHNICAL REPORT DOE AWARD NO. DE-SC0015896

SBIR Phase I

Recipient:	**Particle Beam Lasers, Inc.** **18925 Dearborn Street** **Northridge, CA 91324-2807**
Sponsoring Program Office:	**Division of High Energy Physics** **Office of Science** **U.S. Department of Energy**
Project Title:	**Development of an Accelerator-Quality High-Field Common-Coil Dipole Magnet**
Period of Performance:	**June 13, 2016 through March 12, 2017**
Principal Investigator:	**Ronald M. Scanlan, PBL**
Team Members:	Michael Anerella, BNL Ramesh Gupta, BNL James Kolonko, PBL Delbert Larson, PBL Jesse Schmalzle, BNL Robert Weggel, PBL Erich Willen, PBL

SBIR/STTR Rights Notice

These SBIR/STTR data are furnished with SBIR/STTR rights under DOE Award No. DE-SC0015896 and Brookhaven National Laboratory Strategic Partnership Projects Agreement Number NF-16-24. Unless the Government obtains permission from the Recipient otherwise, the Government will protect SBIR/STTR data from non-government use and from disclosure outside the Government, except for purposes of review, for a period starting at the receipt of the SBIR/STTR data and ending after four (4) years, unless extended in accordance with 48 CFR 27.409(h), from the delivery of the last technical deliverable under this award. In order for SBIR/STTR data to be extended by an STRB/STTR Phase III award, the Recipient must notify DOE's Office of Science and Technical Information (OSTI) before the end of the previous protection period. After the protection period, the Government has a paid-up license to use, and to authorize others to use on its behalf, these data for Government purposes, but is relieved of all disclosure prohibitions and assumes no liability for unauthorized use of these data by third parties. This notice shall be affixed to any reproductions of these data, in whole or in part.

[End of Notice]

Common-Coil Design Concept

This SBIR, a collaboration of Particle Beam Lasers (PBL), Inc. and the Magnet Division of Brookhaven National Laboratory (BNL), advances the technology for a revolutionary type of dipole magnet for colliding-beam accelerators. The design is simpler than traditional cosine-theta magnets and is better at accommodating the lack of ductility of superconductors such as Nb_3Sn needed for field intensities beyond the reach of Nb-Ti.

The research enabled by this SBIR addresses a technological need recognized by the 2014 Particle Physics Project Prioritization Panel (P5) and a recent High Energy Physics Advisory Panel (HEPAP) subpanel [1]. According to P5, US Department of Energy (DOE) research efforts should "Participate in global conceptual design studies and critical path R&D for future very high-energy proton-proton colliders and continue to play a leadership role in superconducting magnet technology focused on the dual goals of increasing performance and decreasing costs". The HEPAP subpanel on Accelerator R&D recommended research to "aggressively pursue the development of Nb_3Sn magnets suitable for use in a very high-energy proton-proton collider" and advocated "simplicity in design for cost reduction" and "development of R&D platforms that reduce turn-around time".

Figure 1 sketches this magnet design, the "common-coil" dipole [2]. Fig. 1a (left) is a rudimentary form, with all coils of simple racetrack shape; Fig. 1b (right) incorporates pole coils, which are allowed to be non-racetrack windings (pink), above and below each beam pipe to improve field homogeneity.

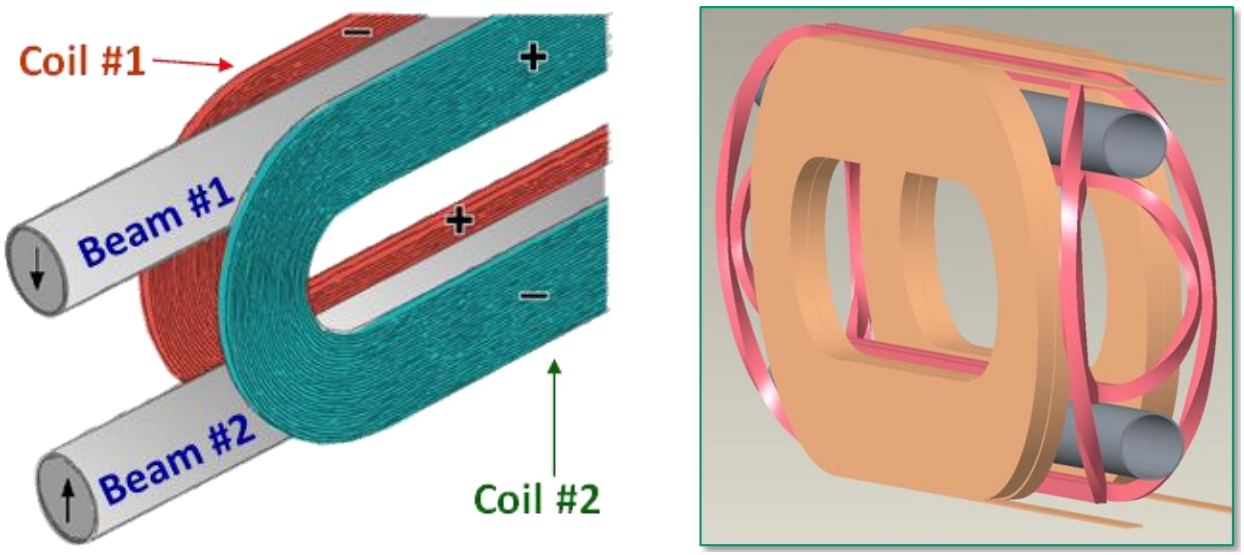

Figs. 1a&b: Illustrative common-coil dipole magnets. Left: A rudimentary design, with two racetrack coils energized oppositely. Plus and minus signs indicate the polarity of current flow; arrows, the field direction in the beam pipes—downward in #1 and upward in #2. Right: With "pole" coils (pink), necessary for accelerator-quality field homogeneity.

In the common-coil design, coils serve two apertures, providing a natural 2-in-1 configuration with fields in opposite directions, as needed in particle colliders. It offers a conductor-friendly design, based on simple racetrack coils with large bend radii, that is particularly suitable for high-field magnets of brittle conductors such as Nb_3Sn and "high-temperature" superconductors

(HTS), which, at temperatures well below that of liquid nitrogen, become *high-field* superconductors. The absence of small-radius bends in the common-coil design allows "react & wind" technology to be used, if preferred, as an alternative to the "wind & react" technology that has been used in a majority of Nb_3Sn dipole and quadrupole magnets.

A great virtue of the common-coil design is that it allows each coil block to move as a separate unit, which reduces stresses and strains on the conductor at the ends. As suggested by Fig. 2a, cosine-theta (and also conventional block-design) magnets tend to be plagued by large stresses and strains on the conductor in the end region. In contrast, the common-coil design (Fig. 2b) allows each coil to move as a separate unit, thus incurring smaller stresses and strains, despite what might be a large displacement of each coil as a unit. Less support structure may suffice, so long as field quality remains adequate. Lowered conductor strain despite reduced structural material may imply better performance as well as lowered cost—both issues in high-field accelerator magnets, where reliability is absolutely essential and magnet structure a major contributor to cost.

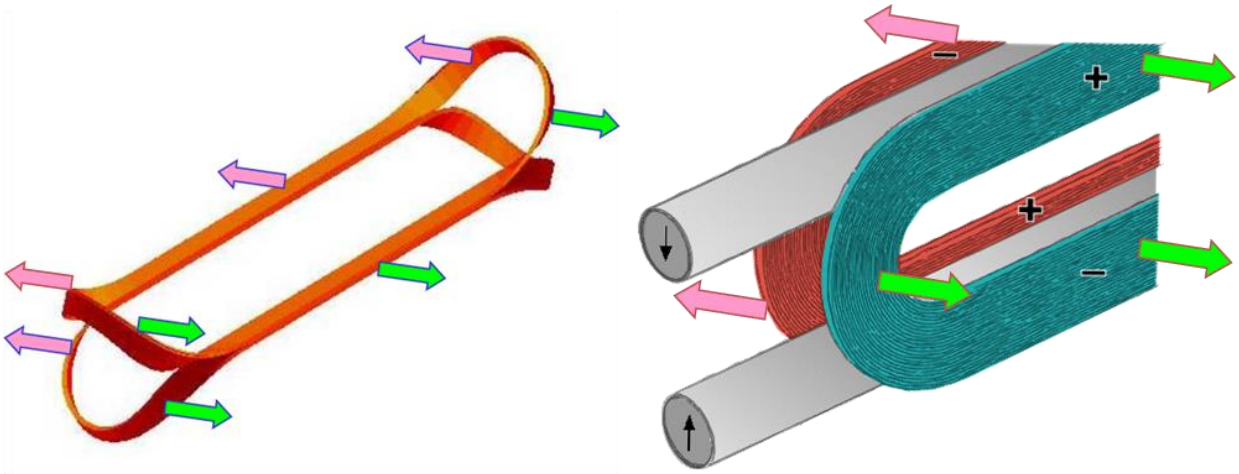

Figs. 2a&b: Lorentz forces in dipole magnets. Left: Cosine-theta (or conventional block-design) magnets typically suffer large internal stresses and strains in the conductor in their end regions. Right: Common-coil magnets may incur lower internal stresses and strains, because each coil moves as a separate unit.

The simpler geometry of the common-coil design allows faster and less-expensive R&D, primarily because of simpler coil-winding and support structure. In various laboratories where R&D magnets based on this design were built and tested [4, 5, 6, 7], the first test results were obtained relatively quickly. In addition, the structure could be modular, and parameters such as coil aperture or individual coil geometry could be changed while retaining most of the other hardware. The same coils built for non-zero aperture magnets could be used as zero-aperture magnets as well, generating higher field. In fact, many common-coil R&D magnets were built with zero gap [4, 5]. Rapid-turn-around, low-cost R&D is a major virtue of common-coil magnets and complies with the recommendation of P5 and its subpanel on accelerator R&D.

Another advantage of the common-coil design accrues from the natural decrease in field from inner layers to outer ones. Significant cost reduction can be achieved by segmenting conductors in a "hybrid" design of high-field and low-field conductors. For a field of 16 T or so, one can run outer layers of NbTi in series with inner layers of Nb_3Sn. To generate even higher field, one can supplement these low-temperature superconductors with HTS.

The common-coil configuration was used in the proposed Very Large Hadron Collider (VLHC) [3] in the USA. Proof-of-principle magnets (Figs. 3 & 4) based on this design were built at several DOE Laboratories [4, 5, 6, 7], including Lawrence Berkeley National Laboratory (LBNL), Fermi National Accelerator Laboratory (FNAL), and BNL.

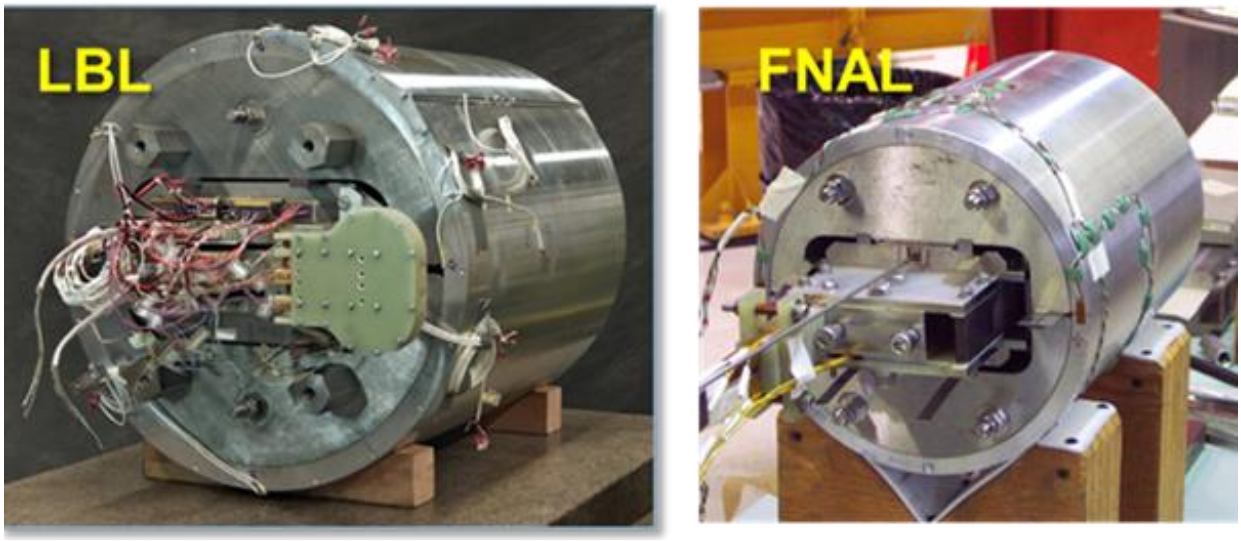

Figs. 3a&b: Two proof-of-principle common-coil magnets. Left: Lawrence Berkeley Laboratory, 2003. Right: Fermi National Accelerator Laboratory, 2003.

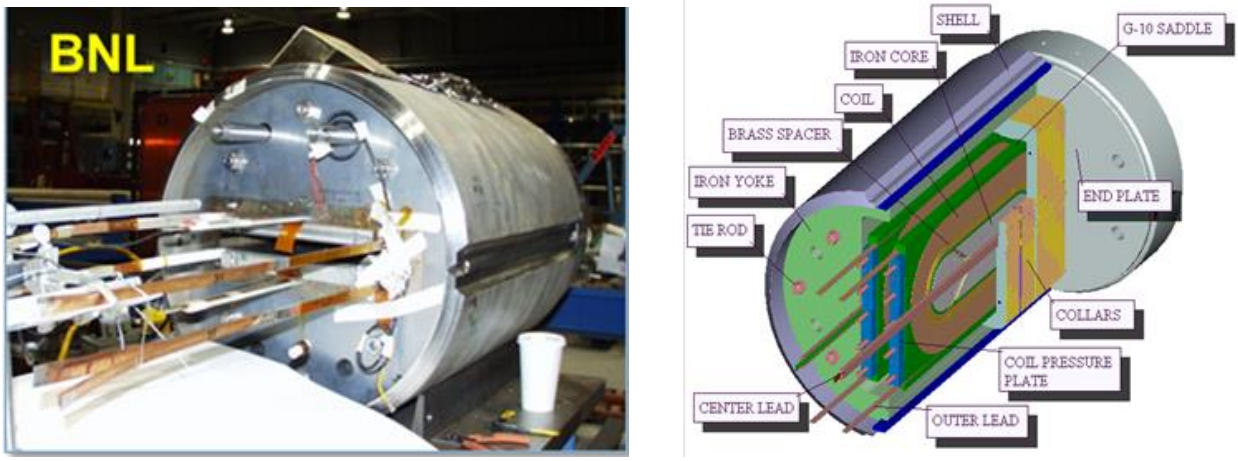

Figs. 4a&b: Proof-of-principle common-coil magnet DCC017 built and tested at Brookhaven National Laboratory in 2006. Left: Photograph, showing cylindrical shell, end plate, multiple current and diagnostic leads, and aperture, 31 mm by ~220 mm. Right: Cut-away schematic with major components labeled.

The very first common-coil test magnet, designed and built [4, 5] while Ron Scanlan, the P.I. for this SBIR, was Program Head at LBNL and Dr. Gupta was the chief designer, reached its short-sample critical current limit without quench. Several subsequent magnets also reached short sample with little or no training. Pre-stress was not needed for good performance; BNL's magnet DCC017 had essentially no vertical or horizontal pre-stress, and yet reached its computed short-sample expectation of 10.2 T. A decade later the magnet was tested again as part of another PBL/BNL STTR and run at 92% of short sample without any quench. The BNL

magnet tolerated displacements computed to be as large as 0.2 mm—much larger than the typical ~25-50 microns allowed in cosine-theta magnets. This exceptional tolerance of conductor motion likely is because the motion is a *displacement*, rather than a *deformation*. Because of this difference, common-coil magnets may require much less structural support than magnets of other types.

Focus of this SBIR

The simple coil geometry of Fig. 1a becomes more complicated with the addition of pole coils—also called pole blocks—that are required to attain the field homogeneity of a few parts in 10^4 needed in accelerator magnets. Conductors in the widely-spaced main coils automatically clear the bore in going from one aperture to the other, but conductors in pole blocks typically do not. To avoid the beam pipe, pole block conductors typically need to veer sideways, violating the simple racetrack coil geometry. To retain racetrack simplicity would require the conductor above beam pipe #1 to return on its own side of the aperture, and likewise for the conductor below beam pipe #2, doubling the number of coils needed, sacrificing some of the simplicity, compactness, and efficiency of the 2-in-1 design.

None of the successful common-coil programs had pole coils, and therefore none produced a design—let alone a magnet—that could provide in a simple and cost-effective manner the high field homogeneity required for accelerator magnets. This SBIR addressed the field-quality issue with new designs using auxiliary coils or pole turns—turns above and below each beam pipe, analogous to those used to shape the field in traditional cosine-theta magnets. Pole turns are technically challenging in common-coil magnets because simple racetrack coils cannot get from one side of a beam pipe to the opposite side. Therefore, the coil ends must be shaped to avoid the beam pipe, yet at the same time have good mechanical support to resist the large Lorentz forces, all while producing good field quality. Ideally, these pole turn coils should be straightforward to fabricate and assemble.

The PBL/BNL team has capitalized upon its advances in coil winding techniques from prior SBIR/STTR-supported projects, plus its fluency with powerful analytical tools such as ROXIE, OPERA, ANSYS, COMSOL and other CAD/CAM programs, to design pole-turn coils. The work developed designs for very high-field Nb_3Sn dipole magnets that are relatively simple and have the potential to be less expensive than competing designs.

In addition, PBL/BNL has used a modern 3-D printer that PBL purchased under another STTR program to print parts to make practice windings.

Benefits of the Common-Coil Design

Proposals by the high energy physics community for proton colliders with a center-of-mass energy up to 100 TeV have reignited interest in designs for magnets that at acceptable cost can generate the field intensity (≥16 T) necessary to fit the collider ring within a pre-existing tunnel or a new tunnel not so long as to be economically prohibitive. CERN hosted a seminar on "Common Coil Magnet Design for High Energy Colliders [8]" for possible use in the proposed Future Circular Collider (FCC) [9]. The common-coil design is the baseline design for the proposed Super proton-proton Collider (SppC) [10] in China.

The research in this SBIR advances the science of building colliding-beam accelerators, benefitting researchers working in high-energy physics around the world. The common-coil design should lower the cost and decrease the complexity of the high-field dipoles required for a Future Circular Collider (FCC). Lower costs are expected because of (a) the simpler geometry and (b) the halving of the number of coils, because each coil serves both beam apertures. The common-coil design is technically appealing for high-field magnets, because each coil module moves as a unit against the large Lorentz forces, reducing the relative motion and internal strain on the conductor.

In indirect ways, the research on developing lower-cost and reliable magnet technology also may contribute to more-immediate practical advances. Compact, high-field superconducting magnet technology may find use in magnetic resonance imaging (MRI), superconducting magnetic energy storage (SMES), proton- and ion-therapy accelerators, and wind-power generation. Although these fields are unlikely to need the common-coil geometry of a colliding-beam accelerator, the above-mentioned advances in superconducting technology gained during the project may prove very important for superconducting magnet technology in general. For instance, advances in the area of stabilizing coils against the Lorentz forces can be important for many applications.

This SBIR developed preliminary engineering designs for 16-T, 50-mm aperture, 2-in-1 accelerator-quality dipoles of Nb_3Sn conductor. It also determined candidate locations for pole-coil conductors within the aperture of the BNL DCC017 common-coil dipole magnet for a proof-of-principle system that could be built and tested within the budget of a Phase II SBIR. The predicted improvement in field homogeneity is a hundredfold, from 220 units (parts in 10^4) over a transverse distance of ±10 mm, to accelerator quality of a few units over that span.

Field Quality Optimization in a Common-Coil Design

Field quality in accelerator magnets is quantified by normal and skew harmonics b_n and a_n:

$$B_y + iB_x = 10^{-4} \times B_{R0} \sum_{n=1}^{\infty} (b_n + ia_n)[(x+iy)/R]^{n-1}, \qquad [1]$$

where B_x and B_y are the components of the field at $[x, y]$, and B_{R0} is the magnitude of the field from the dominant harmonic at a "reference radius" R, typically 17 mm for the magnets designed in this SBIR.

Field-quality optimization in LTS magnets consists of minimizing undesired harmonics, whether of geometric origin, the nonlinearity of the magnetization of iron, or the end (conductor-crossover) regions of the magnet. Achievement of field homogeneity adequate for accelerators requires pole blocks. This SBIR developed accelerator-quality dipole designs with magnets that are less difficult and less costly to build. Figure 5, from a 2000 study [13] of 40-mm aperture dipoles, suggests the variety of designs that can be optimized by the powerful, versatile computer code ROXIE [14] all achieving accelerator-quality field uniformity over the full range of operation in spite of harmonics that creep in from nonlinearity of the magnetization of iron.

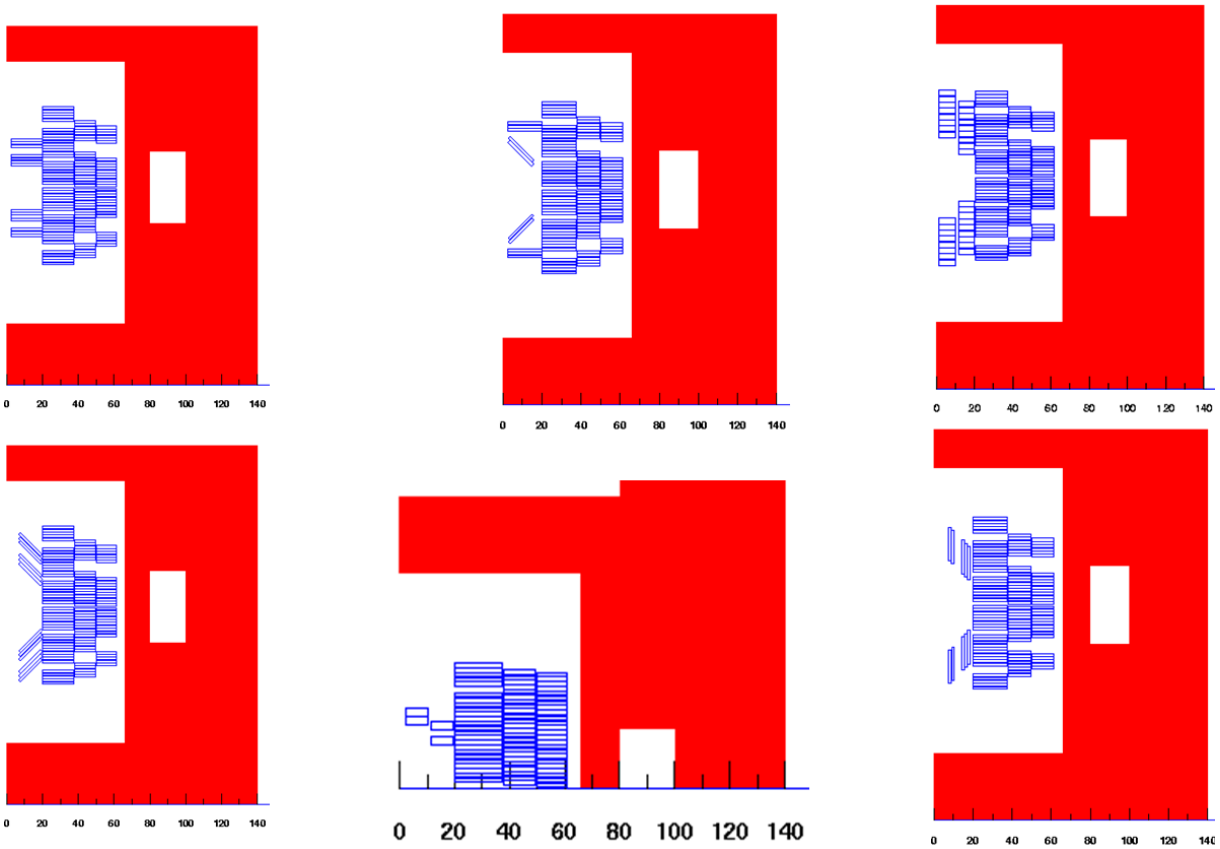

Fig. 5: ROXIE-optimized geometry of conductor turns (blue), magnetic iron (red), and air cavities (right-hand white rectangle) or nonmagnetic stainless steel (other white rectangles) in 40-mm-aperture dipoles to generate accelerator-quality field homogeneity over the full range of operation, despite nonlinearity of iron magnetization.

The remainder of this Final Report addresses the Tasks in the Work Plan of the SBIR Phase I Proposal. In what follows, there is considerable re-emphasis of critical aspects of the design, to enable each description to serves as a stand-alone narrative.

Task 1: Prepare a magnetic design of pole blocks to improve field quality of the DCC017 common-coil magnet

The basic magnetic performance of the BNL common-coil dipole magnet was demonstrated in tests at BNL soon after the magnet's fabrication in 2006. This SBIR employed the powerful design tool ROXIE to determine candidate locations for pole-coils that could improve the field uniformity to accelerator-magnet standards.

The winding pack of the BNL common-coil dipole magnet DCC017 consists of a double-pancake coil separated by a gap of 31 mm from its mirror-image mate on the other side of the magnet aperture. A slice perpendicular to the current flow in the straight legs of each racetrack yields the cross section of Fig. 6a. The field homogeneity (Fig. 6b) is two orders of magnitude shy of accelerator quality, even with a reference radius R of Eqn. [1] of 10 mm (more appropriate for the 31 mm aperture) instead of the 17 mm (appropriate for a 50 mm aperture) used elsewhere in this Report. The harmonic b_3 of Eqn. [1] is huge—188 units—and two other harmonics, b_5 and a_4, also are borderline too large for the field homogeneity desired of accelerator-quality magnets.

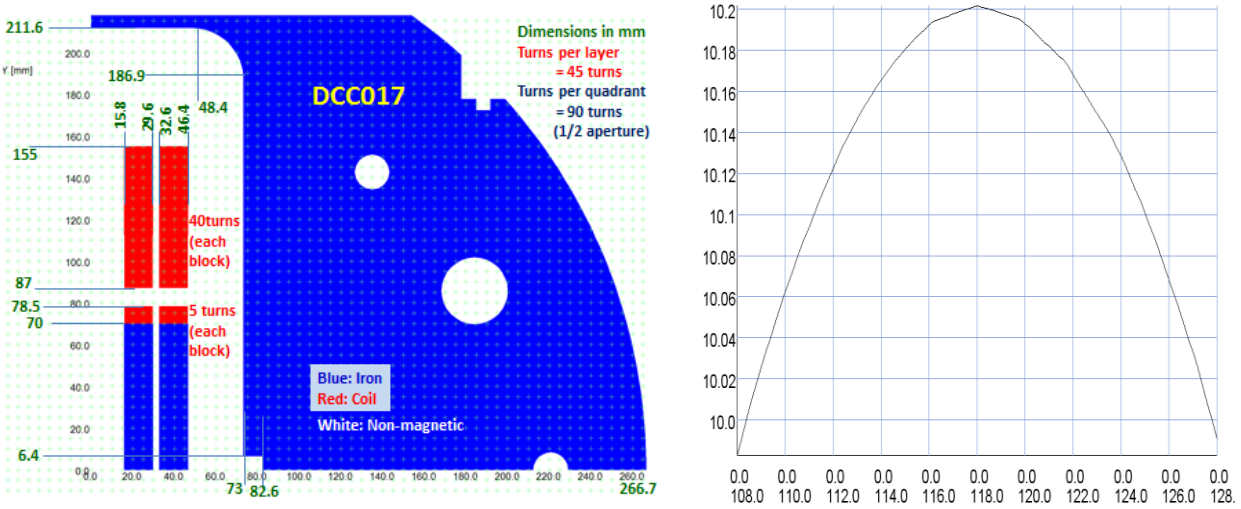

Figs. 6a&b: BNL magnet DCC017 as built. Left: First-quadrant cross section of windings (red) and magnetic iron (blue). Right: Field magnitude along horizontal axis from 108 mm to 128 mm; the field excursion is 0.22 T ≈ 2.2%.

Each of the magnet's four pancakes has 45 turns in two blocks—5 turns and 40 turns—a total of 180 turns of cable 1.7 mm thick by ~12 mm broad. ROXIE analysis found that, conveniently, the same cable suffices for the pole coils as well. Ten turns—two 5-turn pole blocks, one above and one below the midplane, in the configuration of Fig. 7—can bring harmonics close to the specifications of FCC—all harmonics less than 3 units (parts in 10^4) 2/3 of the way to the aperture walls. This capability of pole blocks to produce such a good field quality is remarkable, because field quality was not a consideration in the original design of DCC017. ROXIE analysis was able to upgrade the field quality a hundredfold, even with the cable constrained in size (same dimensions as for the main coil) and orientation (all conductors parallel to each other).

Figs. 7. Partial first-quadrant cross section of windings (blue) and magnetic iron (red) of proposed upgrade to BNL magnet DCC017. Pole coils (small vertical rectangles) improve field uniformity by two orders of magnitude. Inset on right illustrates how pole coils (pink) may clear the beam tubes (gray).

Table 1 lists the computed harmonics at a 10-mm reference radius for the magnet DCC017 at 1 kA, both as-built (left), and (right) with the pole coils of Fig. 7. The as-built magnet has huge harmonics—e.g., b_3 = 188 units, and a_2 = −192 units. The pole coils of Fig. 7 improve the field homogeneity approximately a hundredfold. The largest harmonic is b_7 = 2.7 units; all others are less than 0.4 units. The pole coils also increase the field strength by approximately 7%.

Table 1. Field Harmonics of DCC017 As-Built (left) and with Pole Coils (right)

DCC017 without pole coils (present design)

```
MAIN FIELD (T) ....................................     0.995409
MAGNET STRENGTH (T/(m^(n-1)) ......................       0.9954

NORMAL RELATIVE MULTIPOLES (1.D-4):
b 1:  10000.00000  b 2:      0.00000  b 3:    187.58719
b 4:     -0.00000  b 5:     -2.01358  b 6:      0.00000
b 7:     -0.13995  b 8:     -0.00000  b 9:      0.00365
b10:      0.00000  b11:      0.00136  b12:     -0.00000
b13:     -0.00014  b14:      0.00000  b15:     -0.00000
b16:     -0.00000  b17:      0.00000  b18:      0.00000
b19:     -0.00000  b20:     -0.00000  b

SKEW RELATIVE MULTIPOLES (1.D-4):
a 1:     -0.00000  a 2:   -192.09501  a 3:      0.00000
a 4:      6.49804  a 5:     -0.00000  a 6:      0.33413
a 7:      0.00000  a 8:     -0.03499  a 9:     -0.00000
a10:     -0.00209  a11:      0.00000  a12:      0.00053
a13:     -0.00000  a14:     -0.00002  a15:      0.00000
a16:     -0.00000  a17:     -0.00000  a18:      0.00000
a19:      0.00000  a20:      0.00000  a
```

DCC017 with pole coils (proposed Phase II design)

```
MAIN FIELD (T) ....................................     1.065489
MAGNET STRENGTH (T/(m^(n-1)) ......................       1.0655

NORMAL RELATIVE MULTIPOLES (1.D-4):
b 1:  10000.00000  b 2:     -0.00000  b 3:      0.00071
b 4:     -0.00000  b 5:      0.00045  b 6:     -0.00000
b 7:      2.69589  b 8:     -0.00000  b 9:      0.38260
b10:     -0.00000  b11:     -0.06197  b12:      0.00000
b13:     -0.02446  b14:      0.00000  b15:     -0.00522
b16:      0.00000  b17:      0.00080  b18:      0.00000
b19:      0.00096  b20:      0.00000  b

SKEW RELATIVE MULTIPOLES (1.D-4):
a 1:      0.00000  a 2:      0.00049  a 3:      0.00000
a 4:     -0.00002  a 5:      0.00000  a 6:      0.30753
a 7:     -0.00000  a 8:      0.26673  a 9:     -0.00000
a10:     -0.01777  a11:     -0.00000  a12:     -0.01224
a13:     -0.00000  a14:     -0.00849  a15:     -0.00000
a16:      0.00121  a17:     -0.00000  a18:      0.00129
a19:      0.00000  a20:     -0.00004  a
```

Task 2: Selection of conductor and cable for common-coil magnets

Task #1 determined that, conveniently, the pole coils proposed to be built in Phase II for the BNL common-coil dipole magnet DCC017 could use the same cable as the main coils. Alternative cables being considered use strands of the LHC Accelerator Research Program (LARP) or the upcoming LHC HiLumi upgrade. Both strands are readily available; a cable of ~23 strands could run in series with the DCC017 main coils with a generous critical-current margin.

The Nb_3Sn strands chosen for the several 16-T designs of this Report are those of the EuroCirCol Common Coil [15]. This facilitates comparison of our design with those being studied by CERN and others. Most of our designs utilize cable that is wider than in the EuroCirCol, to increase its short-sample current to ~16 kA at 16 teslas. Increased magnet current implies fewer turns, and therefore less inductance, facilitating better quench protection. It also decreases the number of coils, further reducing magnet cost. That such wide cable can be used is because the common-coil configuration is conductor-friendly in bending.

Conductor strands considered for all the 16-T magnet designs for Phase II are those developed for the LARP (Large Hadron Collider Accelerator Research Program) project. To reduce cost maybe even more, one design uses cable that is identical in strand number as well—LARP cable itself, not merely strand. The cables are rectangular, with Nb_3Sn strands having a diameter of 1.05 mm or 1.1 mm. The ratio of copper to non-copper (superconductor, superconductor precursor, diffusion barriers, etc.) is 1.0 in the inner layer; in the outer layers, it is 1.5, 2.0 or 2.7, depending on the design. The assumed critical current of the superconductor is 1,500 A/mm^2 at 4.2 K and 16 T; a built-in routine of ROXIE deduces the short sample field at 1.9 K. The insulation thickness is 0.15 mm on each side. To facilitate comparison, some designs use the same cable parameters as in the common-coil magnet design study for the EuroCirCol program [12].

Task 3: Prepare a mechanical design of pole blocks to withstand large Lorentz forces and to reduce conductor movement

The simple racetrack geometry and favorable direction of Lorentz forces make the mechanical support of the main common coils reasonably straightforward. However, the pole block coils present more of a challenge, due to the large Lorentz force density (these coils are in the highest field region of the magnet) and the limited space for internal structural support. A particular limitation that is associated only with this proof-of-principle magnet (and not for a new magnet) is how to integrate the new insert coils with the existing main magnet without disassembling it. An internal support structure must fit within the existing aperture and be capable of being inserted into the main magnet without disassembling it.

Sophisticated finite-element-method (FEM) design-and-analysis codes such as ANSYS and COMSOL were used to design structures that satisfy the support requirements. The high Lorentz forces on the pole block coils, acting on superconductor which is brittle, challenge the ingenuity of engineers to provide adequate mechanical support and to facilitate assembly. The vertical (downward) Lorentz forces on the upper and lower blocks of the upper aperture are, respectively, 40 kN/m and 60 kN/m at the maximum operating field; the respective horizontal forces are 530 kN/m and 490 kN/m.

A recent highly-successful test of an HTS/LTS hybrid common-coil dipole built and tested by the PBL/BNL team for a concurrent STTR Phase II [16,17,18] called for a similar structural support. Horizontal Lorentz forces are transferred to the epoxy-fiberglass-impregnated main coils. The vertical forces, which are not as large, are resisted by a stainless-steel structure. Figure 8 shows a conceptual design of mechanical structure to withstand horizontal and vertical forces in the straight section of the insert coil. The general structure is expected to satisfy the structural support requirements of the pole blocks and the constraints of the DCC017 magnet. Pole-coil support for the new magnet will be similar, as in Fig. 9.

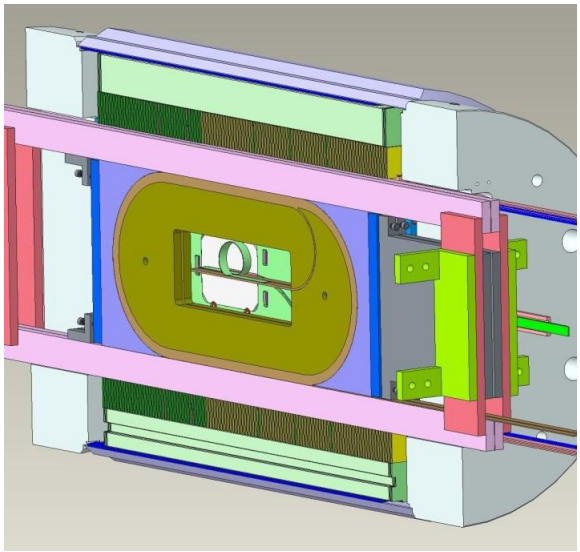

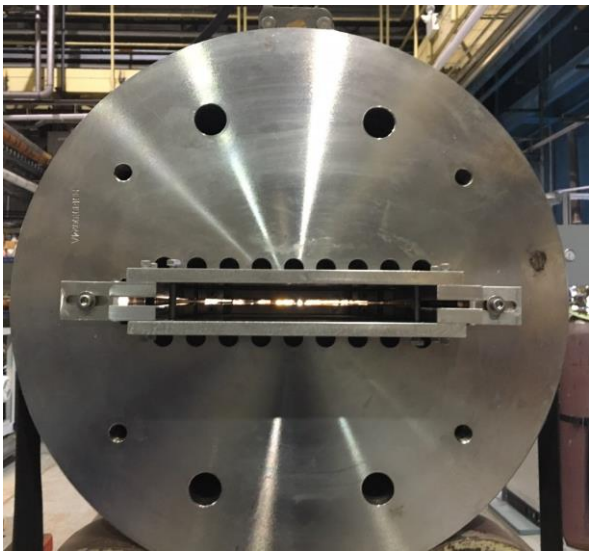

Figs. 8a&b. BNL magnet DCC017 and insert module. Left: CAD drawing highlighting support structure (blue, pink, red) that surrounds the HTS coils (tan) to bear the vertical Lorentz forces. Right: End view of DCC017 magnet and insert module. The HTS coil pair has been spread apart by wedges so that its outboard faces bear against the inboard faces of the main coil; note the light passing through the gap created by spreading the HTS coils.

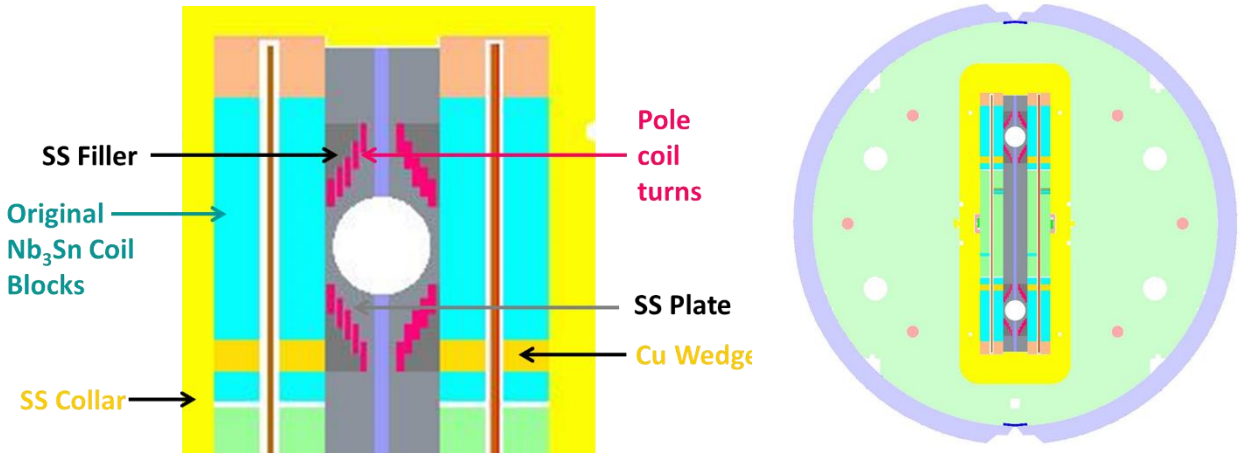

Figs. 9a&b. CAD cross section of support-structure concept, with structure (gray), pole coils (pink), main coils (cyan), wedges & SS collars (yellow), and magnetic iron (pale chartreuse). Left: Detail of support structure for the upper aperture. Right: Cross section through both apertures.

Techniques that also may be investigated include bladders that can increase the preload on these coils after assembly. Also, operating modes that compensate for the relatively large movements of these pole block coils and the main coils will be investigated. Detailed structural design, including end regions, will be carried out using ANSYS and COMSOL early in Phase II.

Task 4: Develop a conceptual design for the assembly and operation of the pole block coils in a common-coil dipole

The basic concept has two machined supports into which the coils would be installed. The supports slide into the aperture with some clearance. Then the supports are forced outward to contact the main coils and a filler installed between the two coil supports (Fig. 9). The design, as mentioned earlier, is based on the successful experience of HTS insert coils in DCC017, with the insert coil package split in the middle. The two insert coils were mechanically forced apart to bear against the main coils after initial assembly and before the 4 K test. This minimized the conductor motion from Lorentz forces pushing the insert coils apart when energized.

In a common-coil design the main-coil conductor is rectangular cable stacked horizontally, returning from one aperture to the other racetrack-wise. Turns in the pole coils pictured in Fig. 7 and Fig. 9 are laid vertically, bending in the easy direction to clear the bore and then returning to the other aperture in a gentle arc. The coils themselves on either side of the aperture (left or right) are allowed to move as a whole, causing little strain in the ends; this is a major benefit of the common-coil design over other designs. The assembly procedure for the Nb_3Sn coils will be similar to that developed for the HTS insert coil for the STTR program. The coil and support structure will be inserted in the bore of DCC017 and the two halves of the pole coils spread apart with a wedge-and-screw mechanism until the pole coils are in firm contact with the main coils (Fig. 8 and Fig. 9).

The preferred mode of operation for the insert coils is to run in series with the main coil. A shunt power supply or a different power supply may be incorporated to allow pole coils to run at a different current from the main coil to deal with a possibly different performance of the two. This choice will be made in the early part of Phase II.

Task 5. Model the coil winding tests

To verify that the coils designed in Tasks 1, 3, and 5 can indeed be wound and supported, a Nb_3Sn cable was obtained from LBNL [19] and used to simulate the coil ends. This cable has 23 strands of 0.8-mm diameter ITER Nb_3Sn; the cable cross section is 10 mm by 1.44 mm. For Phase II, we can use a cable with these dimensions, made from LARP-type Nb_3Sn, and the pole coils operated in series with the main coils with a generous current margin.

As a part of another program, the PBL/BNL team performed some practice winding that is relevant to this SBIR. Figure 10 shows spacers made with a 3-D printer to obtain well-supported ends that satisfy both mechanical and magnetic requirements. Once optimized, the actual spacers to be used in the coil will be metallic, to withstand the temperature needed to react Nb_3Sn.

Figs. 10a&b: Spacers made by a 3-D printer. Left: A quasi-semicircular arc. Right: Complete assembly.

Coil winding structures were made using 3-D printing techniques for fast turn-around (Fig. 10). As a part of another program, PBL purchased a 3-D printer, which avoided high machining costs and allowed parts to be made and a practice coil to be wound within the budget of Phase I. One can see the stairway steps in the printed parts (Fig. 10a), as required for the turns in the design. Fig. 10a shows the winding base before turns are laid in the slot; note the setup for flared ends to clear the bore tube. As mentioned earlier, this pole coil design employs a tight bend radius in the easy-bend direction of the cable, but a radius that is much gentler if bending is in the hard direction. The size limit on parts printed with the PBL 3-D printer limited the size of parts for the model coils, making the task more challenging by forcing us to wind coils with a tighter bend than ideal.

Fig. 11 shows the completed coil winding, demonstrating that the required winding of the cable can be achieved, and that the PBL/BNL team could perform the task in the limited budget of Phase I. A more-detailed engineering design will be performed in Phase II for winding coils with metal parts. Current thinking is that turns will be wound in a metal structure with appropriate wedges for field quality, and then the entire winding will be enclosed in a structure that will be reacted and impregnated.

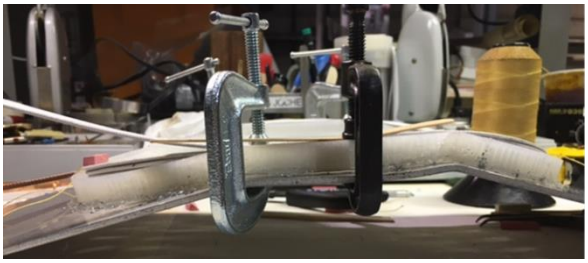
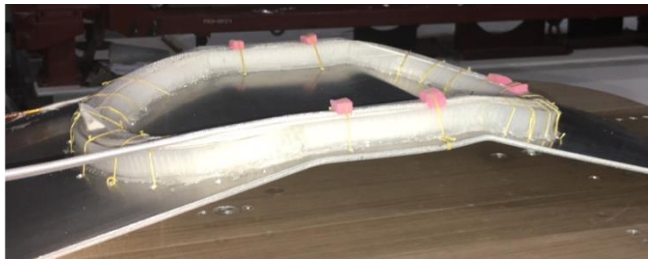

Figs. 11a&b. Photographs of coil winding into Fig. 10 former made by 3-D printing. Left: During the hand winding. Right: Completed winding.

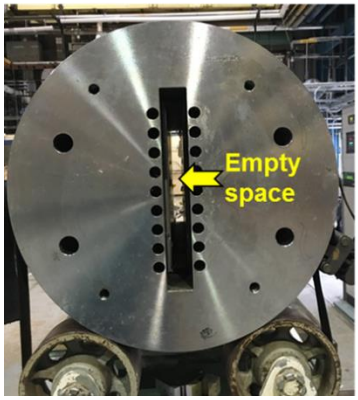

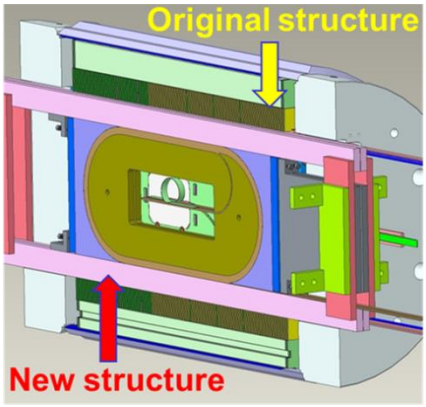

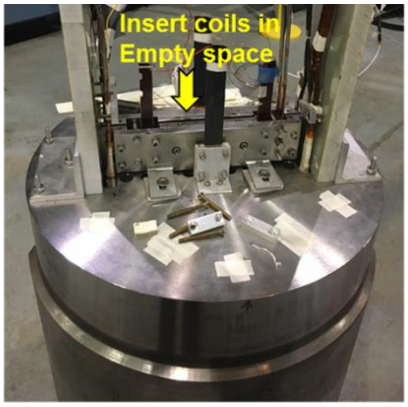

Figs. 12a-c. BNL common-coil dipole DCC017. Left: End view, highlighting the aperture that accommodates new coils without disassembling the magnet. Center: CAD drawing of HTS insert magnet and support structure built and tested very successfully in a concurrent PBL/BNL Phase II STTR for a hybrid HTS/LTS dipole. Right: DCC017 with insert installed.

Task 6. Plan the basic steps required for proof-of-principle tests

Construction of complete pole block coils was beyond the scope of a Phase I effort. However, the basic concept and steps have been developed for a proof-of-principle accelerator-quality dipole with insert coils that can be built and tested in a Phase II. BNL built its Nb_3Sn common coil dipole DCC017 (Fig. 12a&c) with a unique design and structure, with a large open space between the coils (31 mm by ~220 mm). This open space allows coils or coil blocks to be inserted (Fig. 12b) and become part of the magnet without requiring disassembly and reassembly. This approach was used in integrating DCC017 with insert coils (Fig. 12c) and successfully testing the HTS/LTS hybrid as a part of another Phase II. This test and the coil winding tests in Task 5 provide the confidence that pole coils can be added to DCC017.

The new pole coils will be inserted in the DCC017 magnet much like the HTS insert module for the STTR program. However, these proof-of-principle pole coils will differ from those for an accelerator magnet. Pole coils that are flared on both ends would require prohibitively expensive disassembly and reassembly of the DCC017 magnet. Therefore, each of the coils will be flared at only one end, so that its un-flared end can be inserted into the magnet, leaving the flared end protruding beyond the end of the DCC017 magnet. It will still allow the proof-of-principle demonstration and test of flared ends that clear the beam tube, albeit on one side only. A special support structure for the ends will be required. With this, DCC017 will turn into a complete common-coil magnet having not only main coils but also field-shaping auxiliary coils. The

envisioned Phase II effort is expected to be a low-cost, fast-turnaround proof-of-principle demonstration, primarily because DCC017 was designed and built so as to require no major disassembly and reassembly for insert-coil testing. Field measurements will also be performed in Phase II.

Task 7. Plan for the design of a 16-T, 50-mm aperture common-coil for a future proton collider

A very promising design for a 16 T Nb_3Sn common coil dipole has been developed, and was presented to the magnet community at the 2016 ASC conference in September, 2016 [20]. To facilitate comparison, the design used the same strand as that for the EuroCirCol common coil study [15]. The common-coil design allows the use of larger cables, with consequent lower inductance (which facilitates quench protection) and fewer coils (for a less-costly magnet). Several design options were presented, all featuring pole coils inside the main coils of the common coil. These pole coils use relatively little conductor, in a quasi-cosine-theta configuration, to achieve accelerator-quality field. The cross section of one design option is shown in Figure 13; field harmonics—in "units", parts in 10^4—are listed in Table 2.

Design #1

Design #1 is based on the same 1.1-mm strands as those used in the EuroCirCol common coil but employs more strands per cable, to help in quench protection and to decrease the number of coils. The inner layer and pole coils use 36 strands (fewer than the guideline limit of 40), for a width of ~21.3 mm; the outer three layers use 22 strands, for a width of ~13 mm. The cables carry ~16 kA at 16 T.

Numerous coil and yoke iterations with ROXIE [14] optimized the field quality for an aperture-to-aperture spacing of 250 mm and yoke outer diameter of 700 mm, as in the other designs (cosine-theta and block-coil) in the EuroCirCol study; Fig. 13 presents the result. Its peak conductor field is only 0.3% more than at the center of each beam pipe. Table 2 lists the harmonics at the design field of 16 T and reference radius of 17 mm. All harmonics are at least an order of magnitude less than the specification limit of 3 units at the design field of 16 T [15]. Harmonics not listed in the table are zero by symmetry.

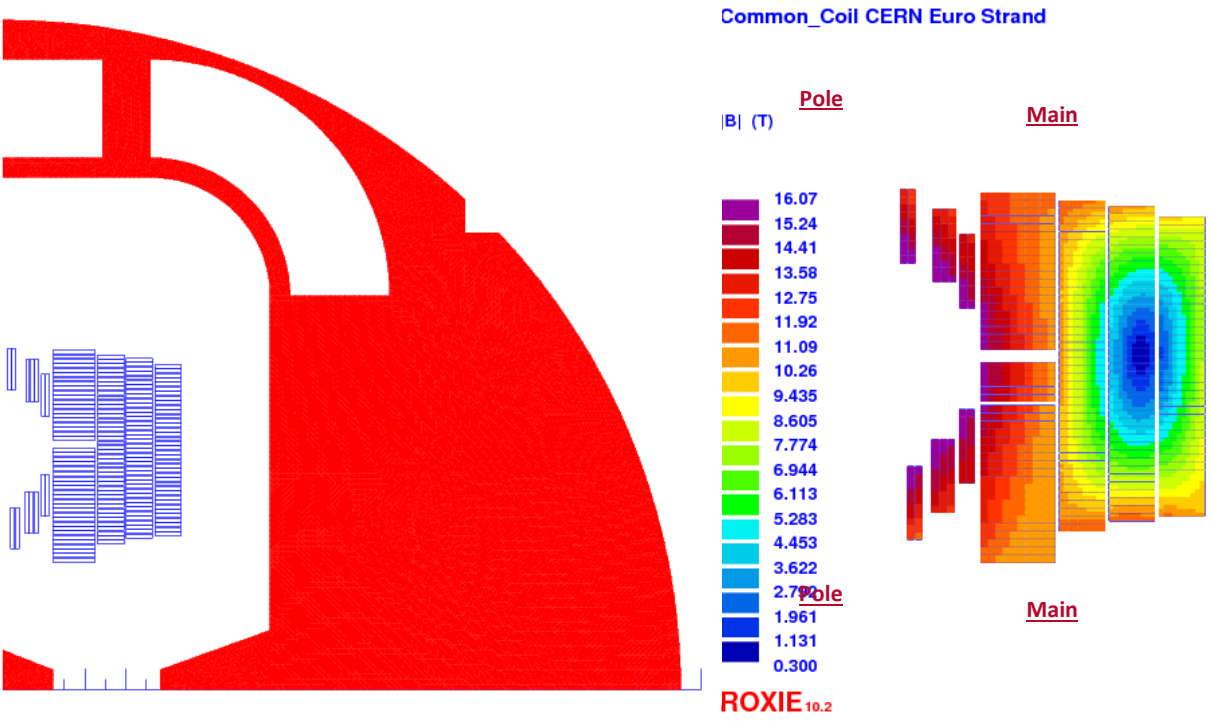

Figs. 13a&b. First-quadrant cross section of 16 T, 50-mm aperture, 2-in-1 common-coil Design #1. Left: Coils (blue), magnetic iron (red), and non-magnetic stainless steel or air cavities (white). Main-coil conductors are stacked vertically; conductors in the pole blocks are stacked horizontally, to bend more easily in veering clear of the beam pipe. Right: Field magnitude, at beam-center field of 16.034 T; B_{max} = 16.5 T.

Table 2: Design #1 Harmonics at 17 mm Radius at 16 T

a_2	a_4	a_6	a_8	a_{10}	a_{12}	a_{14}	a_{16}
0.00	0.00	0.00	0.27	0.21	-0.07	-0.31	0.07
b_3	b_5	b_7	b_9	b_{11}	b_{13}	b_{15}	b_{17}
0.00	0.00	0.01	-0.16	-0.10	-0.35	-0.32	0.03

Figure 14 plots the variation of the harmonics that change significantly with current. Key parameters of the design are given in Table 3. The total number of turns per aperture (which includes turns in both upper and lower coil halves) is 179. It has a stored energy of 1.7 MJ/m per aperture and an inductance of 13 mH/m per aperture.

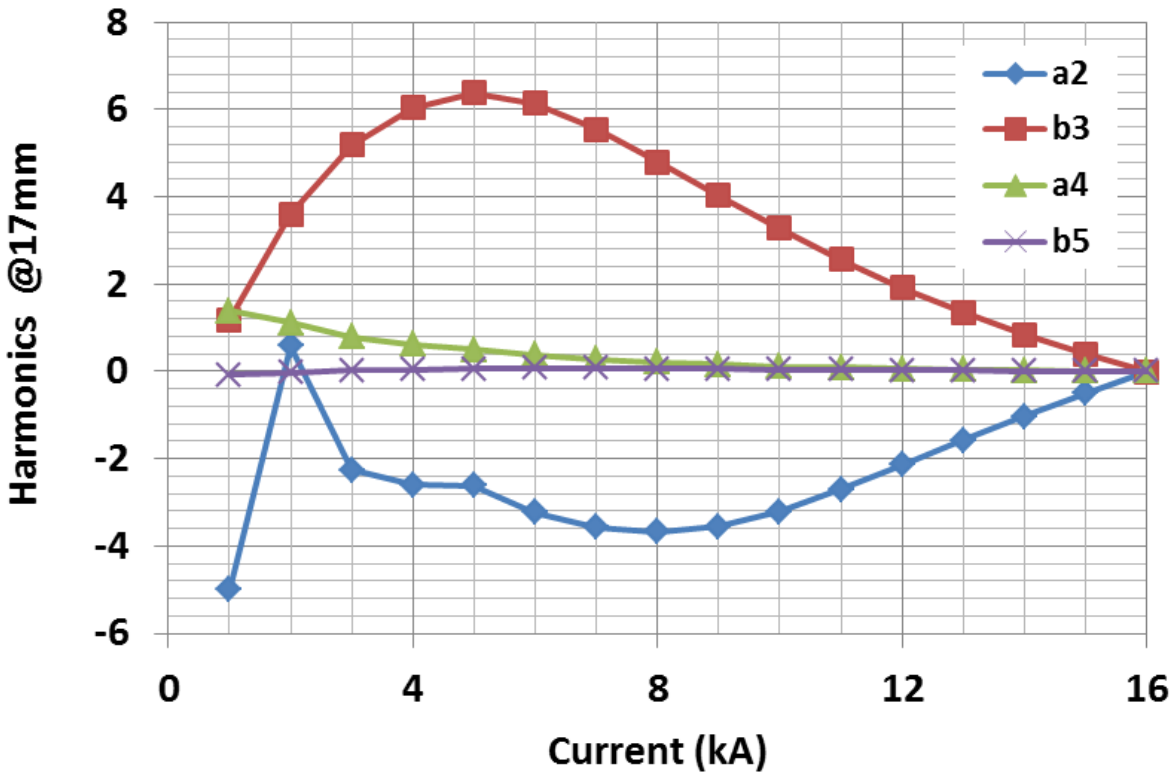

Fig. 14. Current dependence of Design #1 field harmonics at 17 mm reference radius.

Table 3: Parameters of Design #1 (Similar for Design #2)

Operating current	(kA)	15.96
Field in the aperture	(T)	16.0
Margin at 1.9 K	%	19.3
Spacing between beams	(mm)	250
Yoke outer diameter	(mm)	700
Energy per unit length per aperture	(MJ/m)	1.7
Inductance/aperture	(mH/m)	13
Strand diameter (inner & pole layer)	(mm)	1.1
Strands/cable (inner and pole layer)	-	36
Cu/non-Cu (inner and pole layer)	-	1.0
Strand diameter (outer layers)	(mm)	1.1
Strands/cable (outer layers)	-	22
Cu/non-Cu (outer layers)	-	1.5
Total number of turns per aperture		179
Total area of Cu per aperture	(mm^2)	5029
Total area of non-Cu per aperture	(mm^2)	4026
Conductor weight of all FCC dipoles	(tons)	10300

Iron yoke optimization

Iron-yoke optimization was carried out by Nick Maineri, a college sophomore supported by the DOE Science Undergraduate Laboratory Internship (SULI) program [16, 22]. Saturation-induced harmonics were b_3 < 7 units (specification, <10 units) and a_2 < 6 units (specification, <20 units).The fringe field at a radius 150 mm outside the yoke is ~0.25 T with a yoke o.d. of 700 mm, ~0.2 T with a yoke o.d. of 750 mm, and ~0.12 T with a yoke o.d. of 800 mm.

A yoke o.d. of 800 mm yields the best structural stability, magnetic field strength, and field uniformity, including saturation-induced harmonics: b_3 and b_7 can be limited to 6 units each, and b_5 to 5 units. The larger the distance between the iron yoke and the coils in the x direction, the smaller was the change Δb_3 in the b_3 harmonic; a yoke diameter of 800 mm can limit Δb_3 to 6 units. Figs. 15a&b show two candidate designs with a yoke diameter of 800 mm; both limit Δa_2 and Δb_3 to 6 units, the second (step-like) design being the more effective.

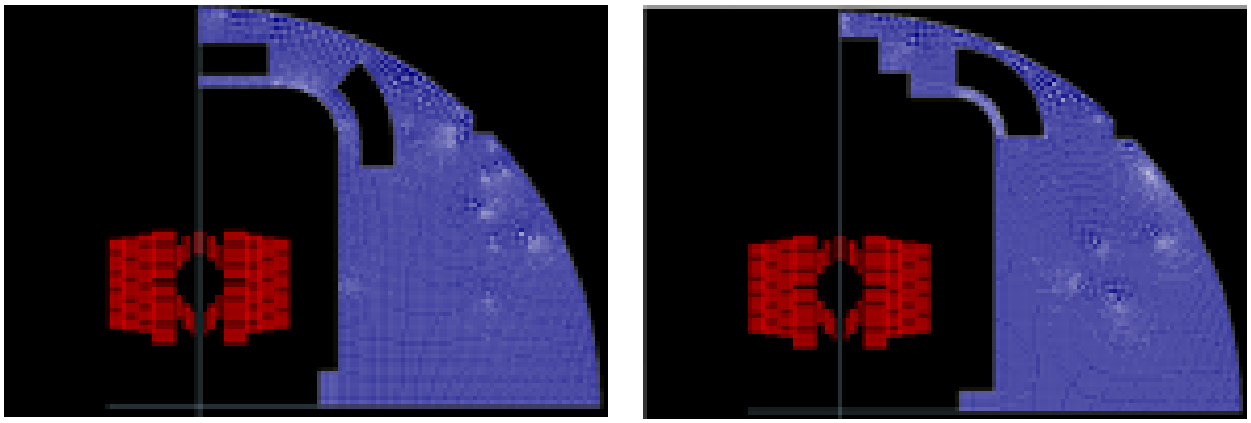

Fig. 15a&b. Two candidate yoke designs of 800 mm o.d. Left: With two holes. Right: With left hole replaced by steps.

The protrusion in the bottom right of the chamber, called a tooth, has a large effect on Δa_2. Early designs for a 700-mm diameter iron yoke included a tooth on the left side, which could limit Δa_2 to 3 units and Δb_3 to 1 unit; later designs abandoned this feature, due to its fabrication complexity.

The largest fringe field occurs between 60° and 70° from the x-axis, depending on the yoke diameter, and is ~1.25 T for 700 mm, 1.0 T for 750 mm, and 0.6 T for 800 mm.

Design optimization #2

Design #2 incorporates 3 mm of support structure outside the pole-coil set to carry Lorentz forces. ROXIE optimization of a few candidate geometries enabled the one pictured in Fig. 16 to meet all specifications (see Table 4). Saturation-induced harmonics and other design parameters remain essentially the same as in design #1—Table 2 and Fig. 14 are valid for Design #2, too, not just Design #1.

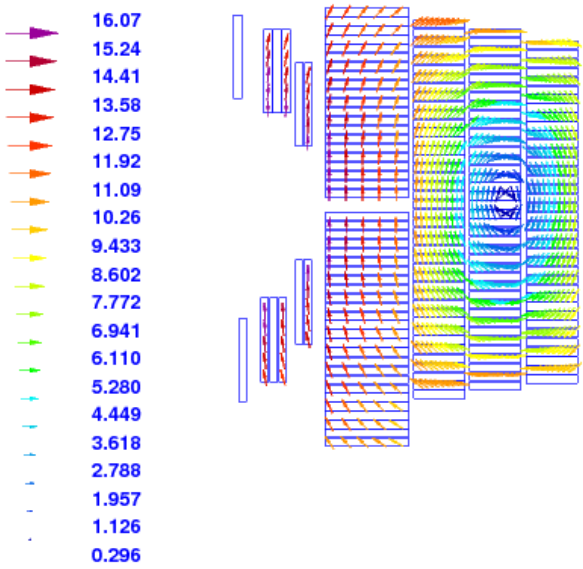

Fig. 16. Windings cross section and field magnitude of Design #2, which includes 3 mm of support structure between the main coils and outermost pole coils to carry Lorentz forces.

Table 4: Design #2 Harmonics at 17 mm Radius at 16 T

a_2	a_4	a_6	a_8	a_{10}	a_{12}	a_{14}	a_{16}
0.00	0.00	0.00	0.00	0.04	-0.89	-0.30	0.19
b_3	b_5	b_7	b_9	b_{11}	b_{13}	b_{15}	b_{17}
0.00	0.00	0.37	2.01	0.10	-1.06	-0.30	0.16

Design optimization #3

Design #3 (Fig. 17) uses strand and cable parameters identical to those used by Toral et al. [17, 23] for the common coil design developed under the EuroCirCol program [12]: strand diameter 1.05 or 1.1 mm, with 12, 14 or 24 strands per cable.

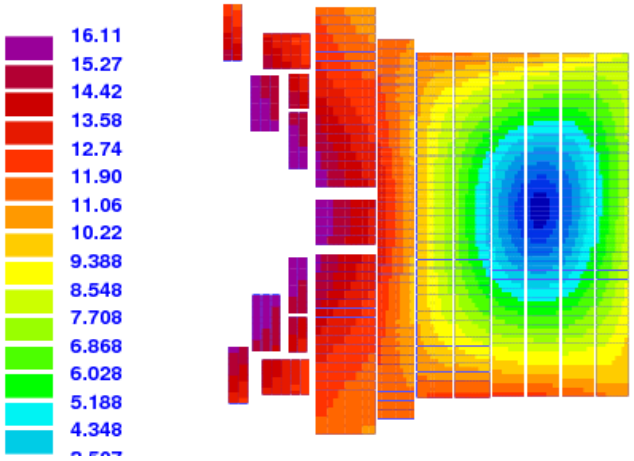

Fig. 17. Winding cross sections and field magnitude of Design #3, which uses the same cable as the EuroCirCol study.

The design generates 16 T field at 8.672 kA, with field harmonics as in Table 5. Examination of more cases should bring b_{11} to within the spec of 3 units. The per-aperture number of turns is 343; the energy per unit length is ~1.8 MJ/m; and the inductance per unit length is ~50 mH/m.

Table 5: Design #3 Harmonics at 17 mm Radius at 16 T

a2	a4	a6	a8	a10	a12	a14	a16
0.00	0.00	0.18	0.82	-0.05	0.15	0.27	0.03
b3	b5	b7	b9	b11	b13	b15	b17
0.00	0.00	0.06	-0.02	4.21	0.26	-0.59	-0.08

Fig. 18a shows the generic geometry of the main coils (tan) and pole coils (pink) in a common-coil design. The main-coil conductor is rectangular cable stacked horizontally, returning from one aperture to the other racetrack-wise. Turns in the pole coils pictured here are laid vertically, bending in the easy direction to clear the bore and then returning to the other aperture along a gentle arc. The coils on either side of the aperture (left or right) move as a whole, causing little strain in the ends, a major benefit of the common coil design.

Fig. 18b shows a simplified two-dimensional ANSYS Workbench model of Design #2. Lorentz forces are applied to the edges of the coil blocks. The collar is monolithic stainless steel, with no joints. The coil windings, Nb_3Sn plus fiberglass impregnated with epoxy, have a Young's modulus of 20 GPa. Frictionless "roller" symmetry is assumed at the horizontal and vertical split lines and also at the outboard edge of the collar, whose thickness is 37 mm.

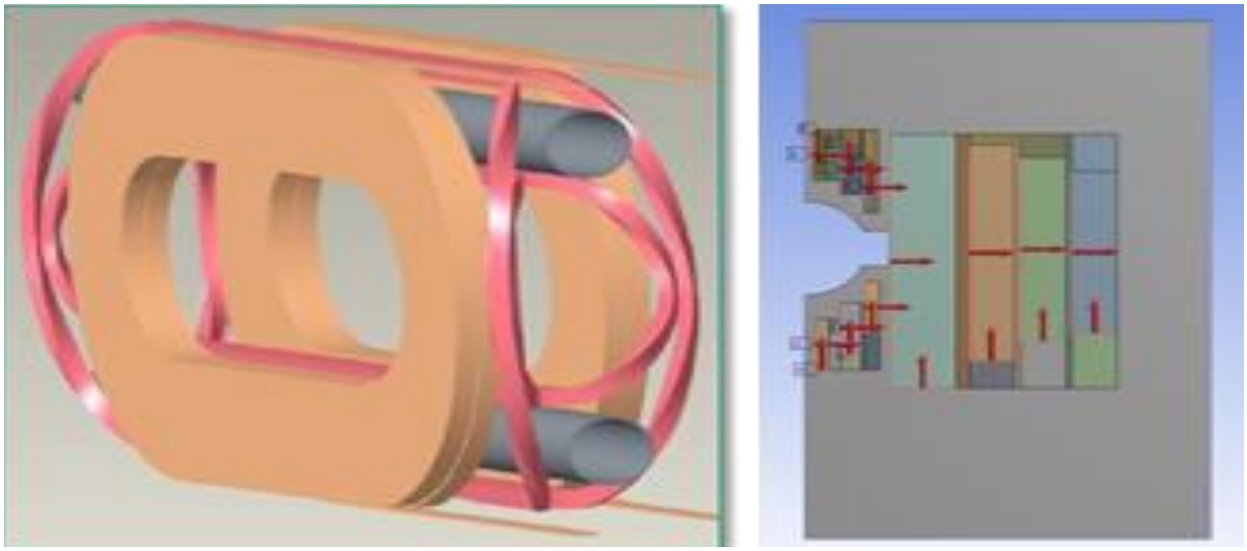

Figs. 18a&b. Geometry and Lorentz forces on common-coil dipole. Left: Generic layout of the main coils (tan) and pole coils (pink). Right: ANSYS model of Design #2, with simplified structure and Lorentz-force application.

Fig. 19a shows the main-coil windings cross sections and stresses, which reach 144 MPa near the midplane of the outermost coil, a value that held even without the roller constraint on the collar. Stresses on the pole coils (Fig. 19b) are below 150 MPa except near the "X" on the right-most pole coil blocks. Future iterations should reduce this value.

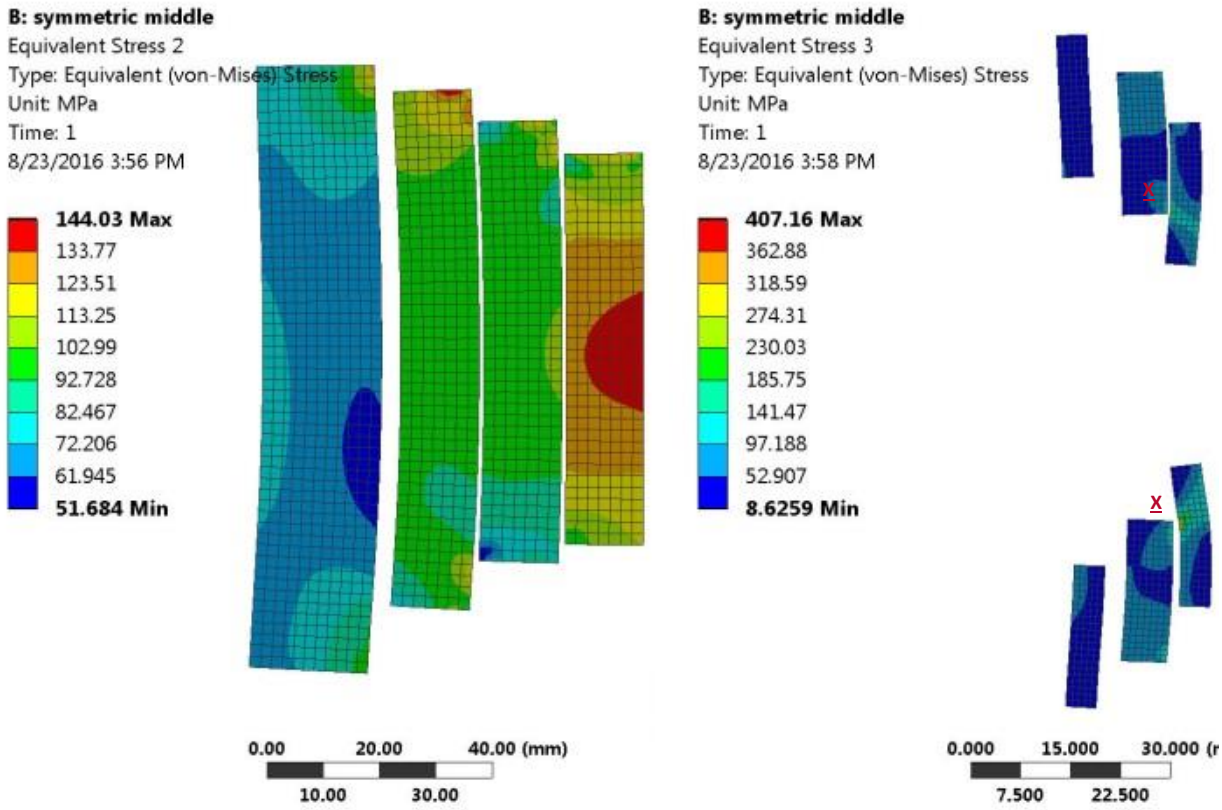

Figs. 19a&b. Windings cross sections and stresses in Design #2 under the simplifying assumptions of Fig. 18b. Left: Main coils. Right: Pole coils.

Figure 20 shows the displacements in the main and pole coils under the Lorentz forces at 16 T. Figure 20a plots the horizontal displacements of the main coils; Fig. 20b, the vertical displacements of the pole coils. The maximum horizontal displacement is ~0.77 mm (in the main coils), which should be acceptable, because each coil moves as a whole (a major benefit of the common coil design), so long as the internal deformations are sufficiently small to keep the strain within the acceptable limit. The horizontal displacement of the pole coil blocks will be limited by the main coils and the support structure. The goal of future iterations will be to make displacements more uniform. The vertical displacements are less than 0.1 mm, which indicates that the support for the pole coils should be able to hold them against the vertical Lorentz forces.

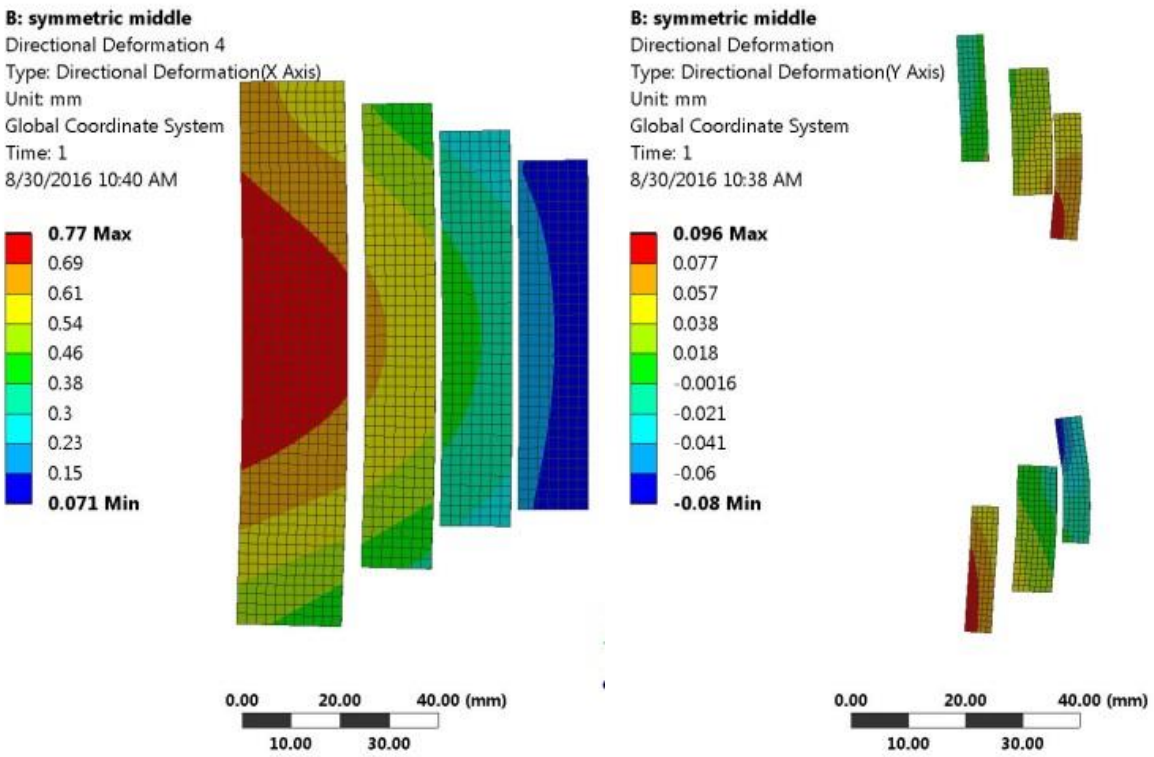

Figs. 20a&b. Displacements of the coils of Design #2. Left: Horizontal displacements of main coils. Right: Vertical displacements of pole coils.

Influence of displacements on field harmonics

Displacements have an impact on field harmonics, and changes in field harmonics may be excessive when the displacements are large. However, changes are expected to be less for displacements that are predominantly horizontal, as here. If all blocks are allowed to move only horizontally, the primary change is Δb_3, with magnitude ~9 units/mm. The field harmonics may also change somewhat due to iron saturation. We expect displacements to be less than 1 mm, and to be able to limit to 10 units the combined effects from displacements and non-linear iron magnetization.

Influence of coil ends on field harmonics

One of the many severe challenges in many magnet designs is obtaining low end harmonics; the common-coil design is no exception. The geometry of ends in a common-coil dipole is unusual in that turns from one aperture typically return to the other aperture. Figure 21 demonstrates that ROXIE could obtain low harmonics [12] despite this asymmetry.

End harmonics in Unit-m

n	Bn	An
2	0.00	0.00
3	0.01	0.00
4	0.00	-0.03
5	0.13	0.00
6	0.00	-0.10
7	0.17	0.00
8	0.00	-0.05
9	0.00	0.00
10	0.00	-0.01
11	-0.01	0.00
12	0.00	0.00
13	0.00	0.00
14	0.00	0.00
15	0.00	0.00
16	0.00	0.00
17	0.00	0.00
18	0.00	0.00

Contribution to integral (a_n, b_n) in a 14 m long dipole ($<10^{-6}$)

n	bn	an
2	0.000	0.001
3	0.002	0.000
4	0.000	-0.005
5	0.019	0.000
6	0.000	-0.014
7	0.025	0.000
8	0.000	-0.008
9	-0.001	0.000
10	0.000	-0.001
11	-0.001	0.000
12	0.000	0.000

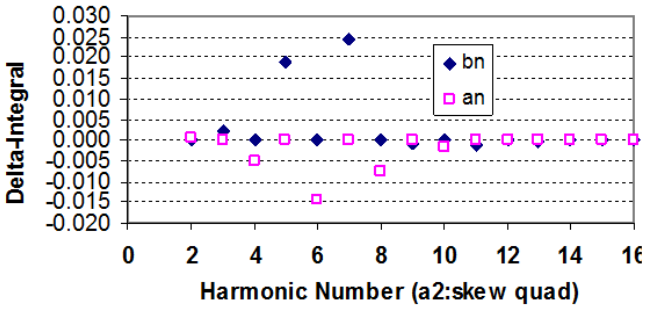

Fig. 21: Optimized magnetic design for ends of a 40-mm aperture common-coil dipole.

Bibliography & References Cited

1. The Particle Physics Project Prioritization Panel (P5) and its subpanel on Accelerator R&D, http://science.energy.gov/hep/hepap/
2. R.C. Gupta, "A Common Coil Design for High Field 2-in-1 Accelerator Magnets," Presented at the 1997 Particle Accelerator Conference in Vancouver, Canada (1997).
3. "Design Study for a Staged VLHC" Fermilab TM-2149 (June 4, 2001) http://tdserver1.fnal.gov/ TDlibry/TD-Notes/VLHC/fermilab-tm-2149.pdf
4. S. A. Gourlay et al., "Fabrication and Test Results of a Prototype, Nb_3Sn Superconducting Racetrack Dipole Magnet," 1999 Particle Accelerator Conference, New York, NY, March 1999.
5. B. Benjegerdes et al., "Fabrication and Test of Nb_3Sn Racetrack Coils at High Field," IEEE Trans. On Applied Superconductivity, 11, March 2001.
6. R. Gupta, et al., "React & Wind Nb_3Sn Common Coil Dipole," 2006 Applied Superconductivity Conf.
7. G. Ambrosio, et al., "Development of a React & Wind Common Coil Dipole for VLHC, Applied Superconductivity Conference at Virginia Beach, USA (2000).
8. R. Gupta, "Common Coil Magnet Design for High Energy Colliders," https://indico.cern.ch/event/442002/Future Circular Collider Study Kickoff Meeting, Geneva, Feb. 12-14, 2014, http://indico.cern.ch/event/282344/timetable/#20140212
9. CEPC/SppC study in China, http://indico.cern.ch/event/282344/session/1/contribution/65/ material/slides/1.pdf
10. R. Gupta, et al., "Field Quality Optimization in a Common Coil Magnet Design," International Conference on Magnet Technology (MT-16) at Ponte Vedra Beach, Florida, USA (1999).
11. https://espace.cern.ch/roxie/default.aspx
12. EuroCirCol – The European Circular Energy-Frontier Collider Study, https://fcc.web.cern.ch/eurocircol/Pages/default.aspx
13. Gupta, R.; Ramberger, S.; Russenschuck, S. "Field quality optimization in a common coil magnet design," Applied Superconductivity, IEEE Transactions on, p 326 – 329, Volume: 10, Issue: 1, March 2000.
14. S. Russenschuck, et al., "ROXIE: Routine for the Optimization of magnet X-sections, Inverse field calculation and coil End design," https://espace.cern.ch/roxie/default.aspx
15. EuroCirCol–TheEuropeanCircularEnergy-FrontierColliderStudy, https://fcc.web.cern.ch/eurocircol/Pages/default.aspx
16. "A Hybrid HTS/LTS Superconductor Design for High-Field Accelerator Magnets", Grant number DE-SC0011348.
17. R. Gupta, et al., "Hybrid High Field Cosine Theta Accelerator Magnets with Second Generation HTS," Presented at ASC 2014, in Charlotte, NC, USA, August 10-15, 2014.
18. R. Gupta, presentation at the Magnet Development Workshop, Napa, CA, Feb. 2017.
19. We are grateful to the LBNL Magnet Group, and Dr. Ian Pong in particular, for supplying this cable.
20. R. Gupta, M. Anerella, J. Cozzolino, W. Sampson, J. Schmalzle, P. Wanderer, J. Kolonko, D. Larson, R. Scanlan, R. Weggel, E. Willen and N. Maineri, "Common Coil Dipoles for Future High Energy Colliders", presented at the Applied Superconductivity Conference, Denver, CO, Sept. 2016
21. D. Tommasini, 1st Review of the EuroCirCol WP 5, "Introduction," https://indico.cern.ch/event/516049/contributions/2029291/attachments/1269286/1882716/WP5Review-Introduction.pdf
22. N. Maineri, DOE Science Undergraduate Laboratory Internship (SULI) program report (unpublished), Summer 2016.
23. Fernando Toral, "Common coil: electromagnetic," https://indico.cern.ch/event/516049/contributions/2029294/attachments/1271104/1883658/Common_coil_electromagnetic_20160511.pdf